THE MULTIPHOTON DISSOCIATION SPECTRUM OF BIS(PERFLUOROISOPROPYL) KETONE

P. A. HACKETT, C. WILLIS and E. WEINBERG

Laser Chemistry Group, Division of Chemistry, National Research Council of Canada, Ottawa K1A OR6 (Canada)

(Received May 21, 1982)

Summary

Multiphoton absorption and dissociation of bis(perfluoroisopropyl) ketone induced by a transversely excited atmospheric pressure CO_2 laser was studied as a function of the wavelength λ and the fluence F of the IR field. The molecule is almost uniquely suited to this type of study: its chemistry is simple allowing unambiguous actinometry and its absorption spectrum is located at the centre of the 10P branch of the $^{13}CO_2$ laser allowing the investigation of the full action spectrum. Both the probability $P_d(\lambda, F)$ of dissociation and the average number $\langle n \rangle(\lambda, F)$ of photons absorbed per molecule were measured at constant pressure (0.5 Torr). The spectral dependence of P_d at constant fluence is a single lorentzian function of halfwidth 5.8 cm^{-1} red shifted 6.0 cm^{-1} from the small signal IR absorption band. The peak for $\langle n \rangle$ is broader (full width at half-maximum of about 14 cm^{-1}), asymmetric and red shifted by only 2.2 cm^{-1}.

1. Introduction

Photolysis in the IR spectral region offers the prospect of molecularly specific excitation and photochemistry. This has been most clearly demonstrated by the many isotope separation schemes devised using this form of excitation [1]. This specificity is particularly significant for large molecules which often have broad featureless absorption bands in other regions so that it is impossible to excite one molecular species selectively in the presence of another.

The molecule 1,1,1,2,4,5,5,5-octafluoro-2,4-bis(trifluoromethyl)-3-pentanone is a large molecule whose chemistry is well suited to actinometric studies of IR multiphoton dissociation. We have investigated the spectral dependence of the dissociation yield. The results are significant in that the dissociation spectrum has a halfwidth (5.8 cm^{-1} at 1 J cm^{-2}) which is less than that of the one-photon absorption spectrum (9.7 cm^{-1}) and is much smaller than its central frequency (1002 cm^{-1}). This yields an effective

0047-2670/83/0000-0000/$03.00

resolution for dissociation by IR frequencies of about 200 which is large compared with that expected in the near-UV region (about 3). This efficient "high resolution" dissociation is significant in terms of the selective dissociation of mixtures and for the specific generation of free radicals.

2. Experimental details

Two parameters were investigated in detail: the single-pulse reaction probability P_d and the average number $\langle n \rangle$ of photons absorbed by an irradiated molecule. These parameters were measured as a function of the irradiating fluence and wavelength. In preliminary experiments the reaction products were analysed by gas chromatography (GC) (9 ft Porapak S; 80 - 100 mesh; copper tubing of outside diameter 1/4 in; 144 °C). Peaks were identified by mass spectrometry analysis of trapped gas chromatographic effluent. The gas chromatograph response was calibrated using authentic aliquots of C_2F_4, C_2F_6 and C_4F_{10}.

Irradiations were carried out in a Pyrex cell (of outside diameter 4.7 cm and length 17.5 cm) equipped with NaCl windows. A Lumonics 101 transversely excited atmospheric pressure (TEA) CO_2 laser modified for closed cycle gas flow and filled with an 80:10:10 He:$^{13}CO_2$:N_2 fuel mix was used [2]. The laser was operated at subatmospheric pressure (625 Torr) to eliminate arcing and to improve the pulse-to-pulse stability (±2%). The beam was apertured to a diameter of 1.4 cm using a carbon iris and was focused at the centre of the cell using a germanium lens of focal length 1 m. Beam intensity profiles were recorded by observing burn patterns of suitably attenuated beams. The arrangement described above ensured that the intensity was constant (±15%) over the irradiated volume. The beam could be attenuated by any of eight NaCl discs (of outside diameter 5 cm and thickness 6 mm) which could be held normal to the beam in rigid optical mounts placed between the lens and the cell. The incident energy was monitored using a pyroelectric detector which viewed the reflected light from the front window. The transmitted intensity was measured using a calibrated pyroelectric detector placed behind the cell which viewed the entire transmitted beam. Analysis of the temporal profile of the intensity using a photon drag detector (Rofin model 7415) revealed the self-mode-locked spike followed by a nitrogen tail typical of gain-switched TEA CO_2 lasers [3].

The extent of the reaction was monitored by the combined measurement of the pressure increase and the pressure of non-condensable (at —196 °C) gas. Pressures were measured using a high precision MKS Baratron capacitance manometer connected to the cell. These pressure values were reduced as previously described to yield single-pulse reaction probabilities [4]:

$$P_d = \frac{\text{number of molecules decomposed}}{\text{number of molecules irradiated}} \quad (1)$$

The values of $\langle n \rangle$ were measured using a partially automated system:

$$\langle n \rangle = \frac{\text{number of photons absorbed}}{\text{number of molecules irradiated}} \quad (2)$$

A CBM 8032 instrument controller issued a command pulse to fire the laser and to trigger sample-and-hold networks built at the National Research Council of Canada. These networks recorded the peak voltage generated by the pyroelectric detectors. These voltages were digitized using an HP3437A scanning digital voltmeter and read into the disc memory of the instrument controller. The laser was not fired on alternate acquisition cycles to allow background correction of the pyroelectric detectors. In a typical measurement two runs were made. In the first run 90 irradiations of the empty cell were made; after every 10 pulses an extra attenuator disc was added to the optical train. A linear least-squares fit of the ratio of the two voltages against the rear pyroelectric voltage was then interpolated and used to calibrate the first detector at the experimental laser frequency. In the second run the cell was filled to the working pressure and a further 90 irradiations were made; after every 10 pulses an attenuator was removed from the optical train. The voltage ratios measured in this run were then combined with the equation determined in the former run to yield the number of joules absorbed in each of the 90 experiments. These values were then converted to values of $\langle n \rangle$ by input of the experimental pressure. Values of $\langle n \rangle$ against the incident fluence F together with a non-linear least-squares fit of these data were then output by the computer.

The principal sources of error in these measurements are noise and voltage drift in the pyroelectric detectors and amplifiers. These result in a ±1.5% precision in the voltage ratio measured at constant fluence for the empty cell. This leads to a ±8% precision in the values of $\langle n \rangle$ (a difference in the voltage ratios). This low precision is offset by the large number of readings and when combined with the calibration accuracy of the rear detector leads to an experimental uncertainty in the reported $\langle n \rangle$ values of ±5%.

3. Results

In all experiments involving parallel beam irradiation it was observed that the rate of increase in total pressure was slightly greater than the rate of increase in pressure of CO ($\Delta P/P_{CO} = 1.10$). This ratio was independent of the excitation frequency, the fluence, the substrate pressure (0.1 - 1.0 Torr) and the pressure of the added gas (up to 1.0 Torr of n-C_4F_{10}). However, the ratio increased with the number of incident pulses ($\Delta P/P_{CO} \rightarrow 1.40$). Moreover reaction probabilities were strongly dependent upon the number of pulses. This latter effect is probably due to the quenching of the multiphoton dissociation by the fluorocarbon reaction products. This was confirmed by experiments in which the reaction probability was measured as a function of added n-C_4F_{10} (Fig. 1). A half-quenching pressure of 0.17 Torr was observed.

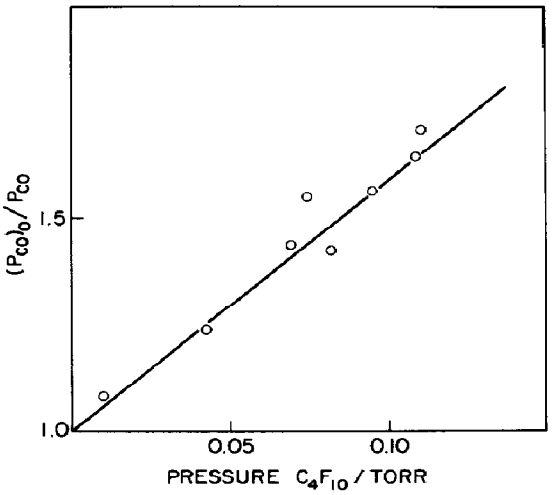

Fig. 1. Effect of added n-C_4F_{10} on the multiphoton dissociation of $(i\text{-}C_3F_7)_2CO$: excitation frequency, 1006.1 cm^{-1}; incident fluence, 1 J cm^{-2}; ketone pressure, 0.5 Torr; temperature, 22 °C; pulse number, 10.

In focused beams the ratio was initially larger ($\Delta P/P_{CO} \approx 2$). This was reflected in the results of GC analysis of the reaction products observed from the two irradiation geometries (Table 1).

In order to avoid the complications introduced by product quenching, secondary photolysis and side reactions all further irradiations were carried out in parallel beams (0.1 - 2.0 J cm^{-2}) at constant ketone pressure (0.5 Torr) and with low conversions (single pulse or below 0.004). The reaction probability was observed to be a simple function of fluence. Figure 2 shows data for irradiation by 1006.1 cm^{-1} radiation (10P(14) $^{13}CO_2$). Table 2 lists the exponents of fluence obtained from plots like Fig. 2 at all wavelengths

TABLE 1

Product distribution from multiphoton IR dissociation of $(i\text{-}C_3F_7)_2CO$

Product	*Rate of formation*[a] (10^{-9} mol pulse^{-1})	
	Parallel[b]	*Focused*[c]
C_2F_6	0.03	1.7
C_2F_4	0.35	8.0
C_4F_{10}	0.52	5.4
C_6F_{14}[d]	2.60	2.2

[a]Pressure of ketone, 0.5 Torr; 1006.2 cm^{-1}; 1.0 J cm^{-2} incident fluence; T = 22 °C.
[b]100 pulses; 3.3 × 10^{-7} mol irradiated per pulse (initial).
[c]50 pulses; 2.6 × 10^{-7} mol irradiated per pulse (initial); beam focused at the centre of the cell by a germanium lens of focal length 10 cm.
[d]GC sensitivity is assumed equal to that of C_4F_{10}.

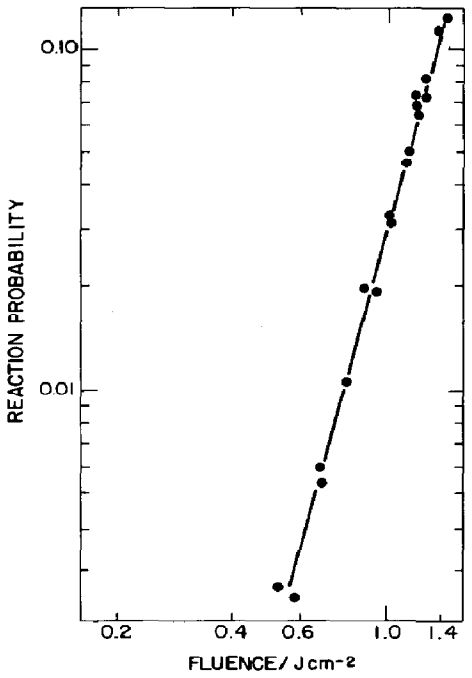

Fig. 2. Effect of incident fluence on the reaction probability: excitation frequency, 1006.1 cm^{-1}; pressure of ketone, 0.5 Torr; temperature, 22 °C.

TABLE 2

Effect of fluence on dissociation probability[a]

Frequency[b] (cm^{-1})	*Fluence range* ($J\ cm^{-2}$)	*Exponent*[c]	*Reaction probability at 1 J* cm^{-2}
1009.5 (10P(10))	0.60 - 0.84	10.3	N.D.[d]
1007.8 (10P(12))	0.65 - 1.10	6.3	0.013
1006.1 (10P(14))	0.56 - 1.40	4.2	0.030
1004.3 (10P(16))	0.89 - 1.25	3.1	0.058
1002.5 (10P(18))	0.56 - 1.12	3.2	0.105
1000.6 (10P(20))	0.86 - 1.05	4.2	0.105
998.8 (10P(22))	0.98 - 1.33	4.4	0.045
996.9 (10P(24))	0.63 - 1.33	6.3	0.018
995.0 (10P(26))	0.95 - 1.17	10.8	0.005

[a]Pressure of ketone, 0.50 Torr; 22 °C; parallel beam irradiation.
[b]$^{13}CO_2$.
[c]Required in the expression reaction probability $\propto$ fluence^n.
[d]N.D., not determined.

studied in this series of experiments. The data in Table 2 are sufficient to give a good description of the reaction probability at all wavelengths and fluences studied here. A graphical representation of the two-dimensional dependence of P_d upon λ and F is shown in Fig. 3.

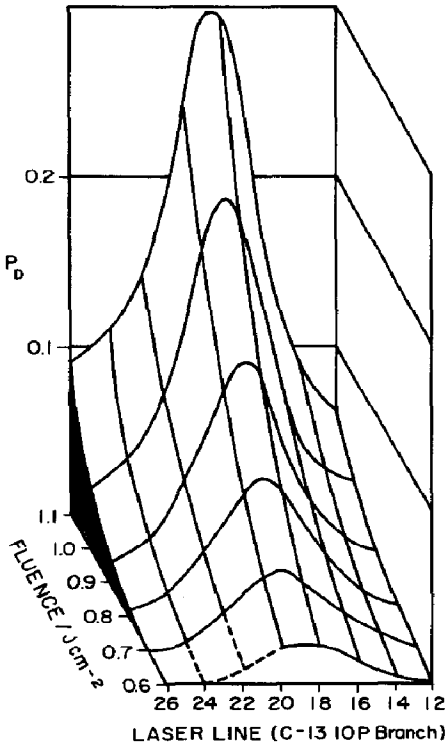

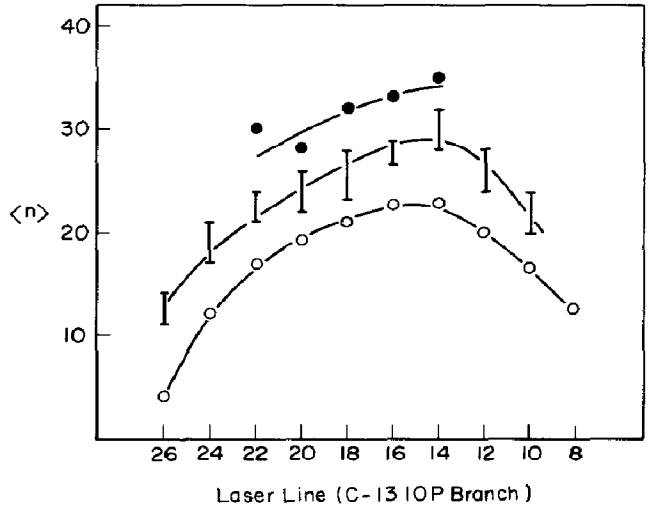

Fig. 3. Effect of the incident fluence and the laser wavelength on the reaction probability. This is a graphical representation interpolated from the data of Table 2.

Fig. 4. Effect of laser wavelength upon $\langle n \rangle$: pressure, 0.5 Torr; temperature, 22 °C. These data were interpolated at three constant fluences (●, 1.4 J cm^{-2}; ⌶, 1.0 J cm^{-2}; ○, 0.6 J cm^{-2}) from experimental data of $\langle n \rangle$ *vs.* fluence at constant laser wavelength as described in the text.

Absorption cross sections were also measured in this work. The data are presented in Fig. 4 where the measured average number of laser photons absorbed is displayed against frequency at three constant fluence values. It is interesting to measure the efficiency of multiphoton dissociation. This can be obtained from the two-dimensional plot of the reaction probability P_d as a function of $\langle n \rangle$ and the CO_2 laser line shown in Fig. 5 for each of the laser wavelengths studied in this work.

4. Discussion

4.1. Reaction mechanism

The observations reported here can be interpreted in terms of the following reaction scheme:

$$(i\text{-}C_3F_7)_2CO \xrightarrow{nh\nu} i\text{-}C_3F_7 + i\text{-}C_3F_7CO \qquad (I)$$

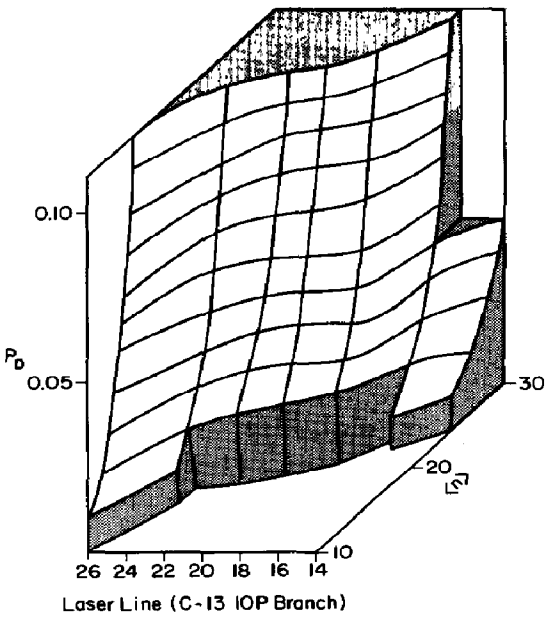

Fig. 5. Efficiency of dissociation: the effect of laser wavelength and $\langle n \rangle$ on the reaction probability: pressure, 0.5 Torr; temperature, 22 °C. This is a graphical representation of interpolated absorption data (see text) and dissociation probability data (Table 2).

$$i\text{-}C_3F_7CO \rightarrow CO + i\text{-}C_3F_7 \quad \text{(II)}$$

$$i\text{-}C_3F_7 \xrightarrow{(nh\nu)} C_2F_4 + CF_3 \quad \text{(III)}$$

$$CF_3 + CF_3 \rightarrow C_2F_6 \quad \text{(IV)}$$

$$CF_3 + i\text{-}C_3F_7 \rightarrow C_4F_{10} \quad \text{(V)}$$

$$2i\text{-}C_3F_7 \rightarrow C_6F_{14} \quad \text{(VI)}$$

Reactions (I) and (II) are analogous to those observed in the multiphoton decomposition of $(CF_3)_2CO$ [3] and the photochemistry of $(C_2F_5)_2CO$ [4] and $(n\text{-}C_3F_7)_2CO$ [5]. Reaction (III) is required to explain the observation of C_2F_4 and C_4F_{10} as reaction products. This reaction could be envisaged as the result of the secondary thermal decomposition of $i\text{-}C_3F_7$ radicals (we note from Fig. 4 that the vibrational temperature of the irradiated substrate is high) or it may be due to secondary photolysis of $i\text{-}C_3F_7$ radicals during the irradiation pulse. An estimate of the threshold energy of reaction (III) can be made from the heats of formation of CF_3 [6], C_2F_4 [6] and $i\text{-}C_3F_7$ [7]; a value of 50 kcal mol^{-1} is obtained which corresponds to only 18 CO_2 laser photons. Secondary photolysis of radical products has been observed for CF_3 [8], C_2F_5 [9] and $n\text{-}C_3F_7$ [10] and cannot be rejected here although the vibrational frequencies of $i\text{-}C_3F_7$ are not known. The pressure increase ratio observed in parallel beams implies that 5% of $i\text{-}C_3F_7$ radicals formed undergo reaction (III) and suggests that reaction (IV) will be unimportant under these irradiation conditions. The data in Fig. 1 can be interpreted in

terms of an average dissociation time constant of the order of the laser pulse width (about 1 μs) if a gas kinetic vibrational relaxation rate constant of 10^{11} l mol^{-1} s^{-1} is assumed. The fact that the dissociation rate, the laser pulse width and the gas kinetic collisional rate at 0.5 Torr are all of the same order will be seen to be relevant to further discussions of the significance of the multiphoton dissociation spectra reported in this work.

4.2. Multiphoton dissociation spectrum

The short discussion presented above indicates that the pressure of CO produced by IR irradiation of $(i\text{-}C_3F_7)_2CO$ serves as an acceptable surrogate for the number of molecules driven to dissociation by the laser field. In this way the situation is analogous to that for $(CF_3)_2CO$ which has a similar multiphoton chemistry [3]. However, for the larger molecule we are able to explore the whole multiphoton dissociation spectrum, whereas for the smaller molecule the limitation in available high power IR radiation frequencies means that we cannot probe the central portion (964.8 - 957.9 cm^{-1}) of the dissociation spectrum. Thus the results reported in Figs. 3 - 6 are among the very few studies of the quantitative spectral dependence of multiphoton dissociation.

The multiphoton dissociation spectrum observed (about 1 J cm^{-2}; 0.5 Torr; 22 °C) can be well represented by a single lorentzian function of half-width 5.8 cm^{-1} whose central frequency at 1002.3 cm^{-1} is red shifted from the peak of the parent one-photon absorption band by 6.0 cm^{-1}. However,

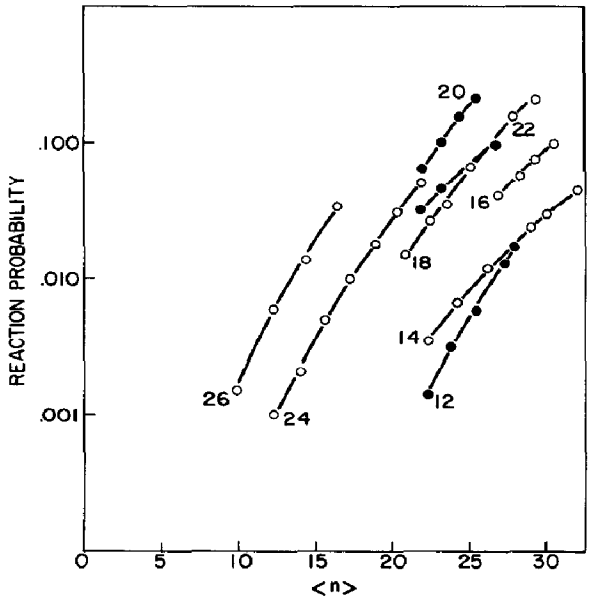

Fig. 6. Efficiency of dissociation: the effect of $\langle n \rangle$ upon the reaction probability at constant laser wavelength (the numbers on the curves represent the 10P branch numbers of the $^{13}CO_2$ laser line; ●, data for P(12), P(20) and P(22)). All the conditions are as for Fig. 5.

we have observed that the reaction probability is strongly dependent upon the incident fluence and frequency (Table 2), the pressure of the added gas (Fig. 1) and the substrate pressure (reaction probability scales as pressure$^{0.5}$ at 1006.1 cm^{-1}). It is evident that the data presented in Fig. 3 contain contributions from many physical and kinetic parameters (transition probabilities, Rabi frequencies, vibrational quenching, rotational relaxation etc.). Obviously spectra obtained under other experimental conditions are needed before detailed comparisons with models of multiphoton decomposition can be made. Indeed most current models of IR multiphoton dissociation have a variety of adjustable input parameters and such comparison may not be worthwhile at this stage. However, the simplicity of the multiphoton dissociation spectrum suggests that a simple mechanism is responsible and in this section we advance a not unreasonable kinetic model to account for the observations.

At all the experimental conditions reported here $\langle n \rangle$ is high as is the reaction probability. Therefore the fraction of molecules interacting with the radiation field must be equally high; it is probable that this fraction tends to unity. This is almost certainly a consequence of the high Rabi frequency encountered during the self-mode-locked spike of the laser pulse. We proceed by assuming that the fraction of molecules interacting with the laser field does not lead to any spectral dependence of $\langle n \rangle$ or P_d. The data in Fig. 3 can then be interpreted in terms of the spectral dependence of the ensemble-averaged multiphoton power absorption. In taking this position we neglect the influence of any energy gap law for rotational relaxation [11] and we assume that all states are coupled by collisions with equal probability.

The problem of multiphoton absorption has received a great deal of theoretical attention. Quantum mechanical [12], quantized classical [13] and classical formulations [14] have been proposed. Lin [13] has shown that these formulations are in exact agreement and predict that the time-ensemble-averaged power absorption $\overline{\langle p(t) \rangle}$ is given by

$$\overline{\langle p(t) \rangle} \propto \frac{\gamma + \Gamma}{(\omega_e - \omega)^2 + (\gamma + \Gamma)^2}$$

i.e. a lorentzian function [13]. γ is the sum of the natural linewidths of the field and the anharmonic-coupling-induced bandwidth for dephasing of the degenerate vibrational levels. The generalized damping factor takes into account all other accumulated line broadening, in particular that due to intramolecular transfer from the optical mode to the heat bath of inactive acceptor vibrational states. This theory was derived from a classical theory of power absorption by an anharmonic oscillator with effective (power-dependent) frequency ω_e [13]. Theory and experiment are thus in agreement: neither give a positive identification of the source of the line broadening, dephasing or intramolecular energy transfer. In the absence of spectroscopic parameters for the molecule under study and of a full dynamic and kinetic theory of multiphoton absorption and dissociation, further comparison would appear to be unwarranted. However, we note that Chou and Grant

[15] have recently inferred that the multiphoton dissociation spectrum of CF_2Cl_2 is well represented by a lorentzian function centred at the Q branch maximum of the one-photon absorption transition. They calculate "relaxation rates for molecules at a level critical for continued IR multiphoton absorption of 100 ps and 5 ps at room temperature and 150 °C respectively".

However, our data cannot be interpreted in an analogous manner. We observe that distributions of vibrationally excited molecules characterized by $\langle n \rangle \approx 30$ still yield a spectral dependence for P_d which does not mirror that for $\langle n \rangle$. Thus a model in which the spectral dependence of both $\langle n \rangle$ and P_d is due to the power absorption of a state at the entrance to the vibrational quasi-continuum cannot be invoked in this case. Furthermore the data of Figs. 3, 4 and 7 which show a marked spectral dependence of P_d over frequencies where $\langle n \rangle$ varies only from 18 to 22 (at 0.6 J cm^{-2}) imply that even states with a high degree of vibrational excitation do not contribute to the spectral dependence of P_d.

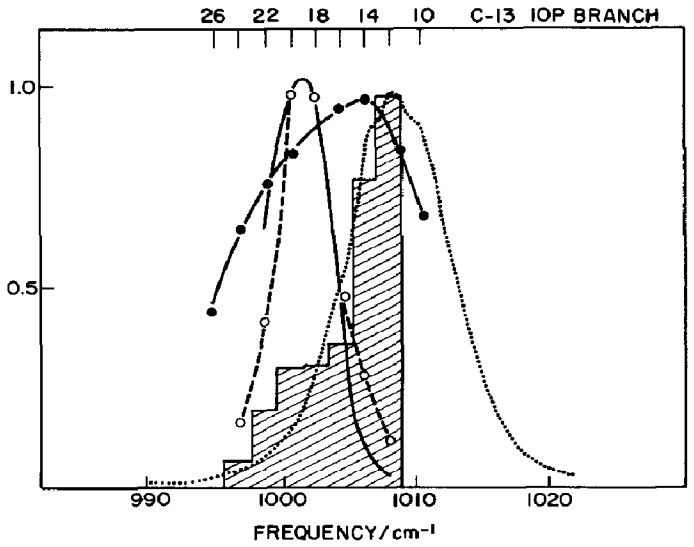

Fig. 7. Spectral dependence of $\langle n \rangle$, P_d, $\sigma(\lambda)$ and $A(F, \lambda)$ (see text). The data are presented as peak-normalized spectra against frequency: ·····, small signal Fourier transform IR absorbance spectrum; ●, $\langle n \rangle$ at 1 J cm^{-2}; ○ P_d at 1 J cm^{-2}; ——, $\sigma(\lambda)$ derived from data at $\langle n \rangle = 22$ and $\langle n \rangle = 24$; the histogram represents $A(F, \lambda)$ derived from $\sigma(\lambda)$ and P_d data at 1.25 J cm^{-2}.

A model consistent with the observations and qualifications presented above would involve a competition between photon absorption (leading to dissociation) and vibrational relaxation (quenching) for excited molecules which lie very close to the dissociation threshold. The degree of excitation for the molecules postulated in this model would be such that the Rice–Ramsperger–Kassel–Marcus (RRKM) spontaneous dissociation rate just becomes competitive with the collisional relaxation rate; absorption of very few more photons would lead to states where the RRKM dissociation rate dominates the collisional rate. In order to observe this competition it is

necessary that the rate of photon absorption (determined by the flux and the cross section) is not so high as to dominate the kinetics, *i.e.* the point where photon absorption dominates vibrational relaxation and is only terminated by the increasing dissociation rate constant. The observations of the magnitude of the global dissociation rate reported in the previous section are consistent with this postulated kinetic situation.

If the kinetic situation described above pertains then the spectral dependence of P_d at constant fluence is due both to the power absorption spectrum of the threshold molecules and to the spectral dependence of their production. Thus

$$P_d(F, \lambda) = \frac{A(F, \lambda)F\sigma(\lambda)}{F\sigma(\lambda) + Q} \tag{3}$$

where $A(F, \lambda)$ represents the fractional probability of population of threshold states, $\sigma(\lambda)$ represents the absorption cross section of such states (here we neglect any power dependence of that absorption cross section) and Q is a constant representing the global quenching rate.

The spectral dependence of $\sigma(\lambda)$ can be examined if we make the assumption that the distribution function of vibrationally excited molecules is independent of excitation wavelength, *i.e.* experiments leading to equivalent $\langle n \rangle$ values produce identical distributions of vibrationally excited molecules ($A(F, \lambda) \propto \langle n \rangle$). This assumption replaces and does not require the assumption discussed earlier that the fraction of molecules interacting with the laser field at constant fluence has no spectral dependence. If the data are then inspected at constant and low values of $\langle n \rangle$ so that $F\sigma(\lambda)$ is less than Q, we have

$$P_d(F, \lambda) \propto F\sigma(\lambda) \qquad \langle n \rangle = \text{constant} \tag{4}$$

Our data allow us to make this inspection at $\langle n \rangle = 22$ and $\langle n \rangle = 24$. The resulting spectra of $\sigma(\lambda)$ are equivalent at both $\langle n \rangle$ values and are shown in Fig. 7. We can now investigate the spectral dependence of $A(F, \lambda)$ by substituting $\sigma(\lambda)$, whence we obtain

$$P_d \propto \frac{A(F, \lambda)}{\sigma(\lambda)} \qquad F = \text{constant} \tag{5}$$

The results of this manipulation at $F = 1.25$ J cm^{-2} are also shown in Fig. 7 as the histogram of values of A. We should comment upon the quality of the data. $\langle n \rangle$ is only known to a precision of 5%. This uncertainty is similarly reflected in the value of the fluence leading to constant $\langle n \rangle$ and is magnified by the exponent of fluence listed in Table 2 in defining the P_d values at constant fluence. Thus the total uncertainty in the values of $\sigma(\lambda)$ and $A(F, \lambda)$, calculated through eqns. (4) and (5) respectively, is of the order of $0.05(n - 1)$ where n is the exponent of fluence listed in Table 2. Clearly, to carry this analysis further more precise $\langle n \rangle$ values are required. There appear to be no simple experimental solutions. Higher net absorptions cannot be used and the precision of energy ratio measurement is already high.

Given the reservations noted above, the $\sigma(\lambda)$ and $A(F, \lambda)$ spectra are not physically unreasonable. The absorption spectrum of threshold molecules $\sigma(\lambda)$ appears strongly red shifted (by about 6.0 cm^{-1}) from the small signal absorption spectrum and its extrapolated halfwidth (about 6.5 cm^{-1}) can most reasonably be assigned as due to homogeneous line broadening (intramolecular vibrational redistribution on the 10^{-12} s time scale). The form of $A(F, \lambda)$ parallels the small signal absorption spectrum. This is reasonable in the limit of low Rabi frequency as the small signal spectrum really represents a population distribution of resonant states. This distribution must also affect the spectral dependence of interacting states at intermediate intensities and is only negligible at high Rabi frequencies.

The simplistic model presented above is an attempt to explain the significant observation that the spectral dependence of P_d is narrower than that for $\langle n \rangle$. The model encompasses the assumption that the high intensities of the laser field of the self-mode-locked CO_2 laser spike raises a subset of molecules into the quasi-continuum and that this subset of molecules is driven to dissociation by the lower intensities characteristic of the tail of the pulse. Two other models can be discussed and the data of Fig. 6 can be used to reject one of them. A purely collisional thermal model can be rejected because the data in Fig. 6 clearly show that the dissociation yield is not solely dependent upon the amount of energy deposited into the gas, *i.e.* upon $\langle n \rangle$. Clearly red frequency irradiation is more efficient than blue frequency irradiation. This difference, which is obviously a consequence of molecular anharmonicity, can be accounted for by a third model. This model would invoke the full internal energy dependence of the quasi-continuum absorption [16]. For red-edge excitation increased excitation would tend to make molecules more resonant with the field, whereas for blue-edge excitation anharmonicity would require that the molecule–field interaction would become more non-resonant and the pumping rate would decrease as the internal energy increased. Thus the distribution function of vibrationally excited molecules may depend upon the excitation frequency and the assumption used to derive eqn. (4) ($A(F, \lambda) \propto \langle n \rangle$) may not be valid. A full treatment of this model is not warranted. However, we note that the broad spectral dependence of $\langle n \rangle$ reported in Fig. 4 does not really support this contention.

4.3. Selective molecular dissociation

Although the interpretation of the multiphoton dissociation spectrum is necessarily ambiguous, its significance for selective dissociation of large polyatomic molecules is clear. $(i\text{-}C_3F_7)_2CO$ may be dissociated with high efficiency (0.20) in beams of moderate fluence (1 J cm^{-2}) whenever the incident radiation frequency is in the range 990 - 1015 cm^{-1}, but will not be dissociated at other frequencies accessible to the CO_2 laser. Other workers have reported the generation of C_3F_7 radicals by IR multiphoton dissociation of C_3F_7Br and C_3F_7I [10]. In these cases the secondary photolysis of C_3F_7

radicals was a major reaction pathway. We attribute this difference in behaviour to differences in irradiation frequency and note that it should always be possible to choose radical precursors that can be photolysed at IR frequencies far removed from free-radical absorption bands.

The present molecule therefore serves as a good source of i-C_3F_7 radicals in the same way as hexafluoroacetone does for CF_3 radicals [3].

Acknowledgments

We should like to thank Dr. Chou and Dr. Grant for communicating their results on CF_2Cl_2 to us prior to publication.

This work has been issued as *NRCC Rep. 20557* (National Research Council of Canada).

References

1 J. L. Lyman, G. P. Quigley and O. P. Judd, in C. Cantrell (ed.), *Multiple Photon Excitation and Dissociation of Polyatomic Molecules*, Springer, Heidelberg, 1979.
2 C. Willis, P. A. Hackett and J. M. Parsons, *Rev. Sci. Instrum., 50* (1979) 1141.
3 P. A. Hackett, C. Willis and M. Gauthier, *J. Chem. Phys., 71* (1979) 2682.
4 G. Giacometti, H. Okabe, S. J. Price and E. W. R. Steacie, *Can. J. Chem., 38* (1968) 104.
5 G. H. Miller, G. O. Pritchard and E. W. R. Steacie, *Z. Phys. Chem., 15* (1958) 262.
6 D. R. Stull and H. Prophet (eds.), *JANAF Thermochemical Tables*, in *NBS Natl. Stand Ref. Data Ser. 37*, 2nd edn., 1971 (National Bureau of Standards, U.S. Department of Commerce).
7 W. M. D. Bryant, *J. Polym. Sci., 56* (1962) 277.
8 E. Wurzberg, L. J. Kovalenko and P. L. Houston, *Chem. Phys., 35* (1978) 317.
9 E. Weinberg, M. Gauthier, P. A. Hackett and C. Willis, *Can. J. Chem., 59* (1981) 1307.
10 M. J. Rossi, J. R. Barker and D. M. Golden, *J. Chem. Phys., 76* (1982) 406.
11 R. B. Kurzel, J. I. Steinfeld, D. A. Hortzenbuhler and G. E. Leroi, *J. Chem. Phys., 55* (1971) 4822.
12 L. M. Narducci, S. S. Mitra, R. A. Shatas and C. A. Coulter, *Phys. Rev. A, 16* (1977) 247.
13 J. Lin, *Phys. Lett. A, 70* (1979) 195.
14 T. P. Cotter, W. Fuss, K. L. Kompa and H. Stafast, *Opt. Commun., 18* (1976) 220.
15 J. S. Chou and E. R. Grant, *J. Chem. Phys., 74* (1981) 384.
16 J. W. Hudgens and J. R. McDonald, *J. Chem. Phys., 76* (1982) 173.